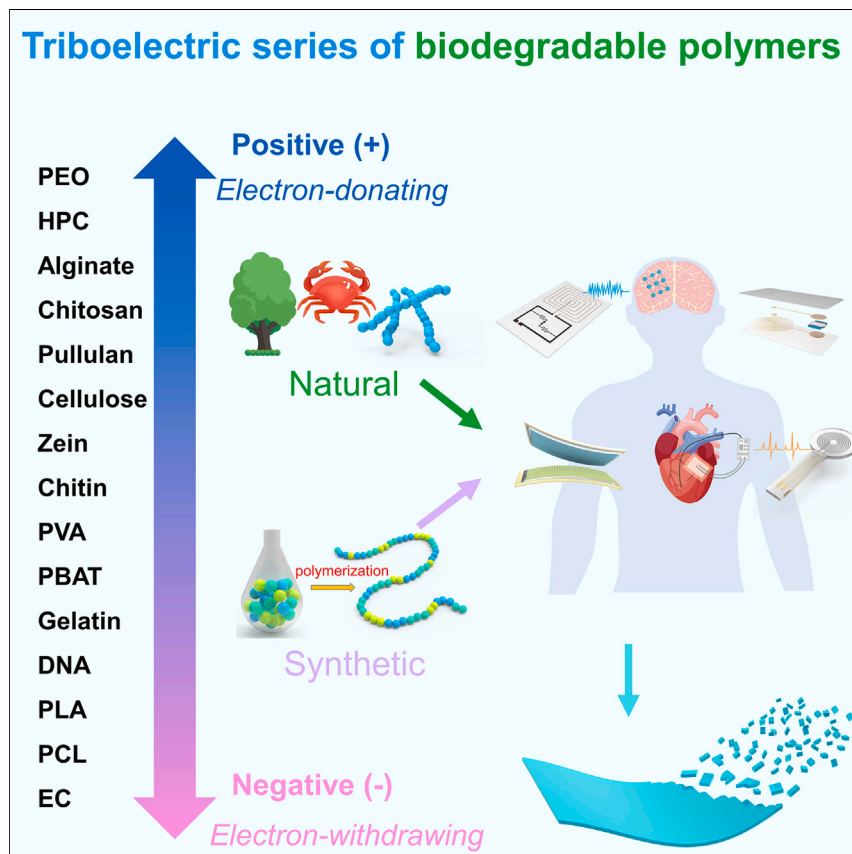


Article

Triboelectric performances of biodegradable polymers



We developed a triboelectric series of a comprehensive range of biodegradable polymers (BPs) by ordering the triboelectric polarities of different BPs according to the transferred charge results and innovatively summarized and analyzed the regularities and principles of influence of various main- or side-chain chemical groups on the triboelectric polarity of BPs.

Hongyu Meng, Qiao Yu, Zhuo Liu, ..., Xianzhu Yang, Zhong Lin Wang, Zhou Li

zli@binn.cas.cn

Highlights

Comprehensive range of triboelectric BP films are prepared and tested in a uniform state

Developing a triboelectric series of 40 kinds of biodegradable polymers

Summarizing influences of various chemical groups of BPs on triboelectric polarities



Understanding

Dependency and conditional studies on material behavior

Article

Triboelectric performances of biodegradable polymers

Hongyu Meng,^{1,3,13} Qiao Yu,^{1,2,13} Zhuo Liu,^{1,4,13} Yansong Gai,^{1,2} Jiangtao Xue,¹ Yuan Bai,^{1,2} Xuecheng Qu,^{1,3} Puchuan Tan,^{1,3} Dan Luo,^{1,2,3} Wenwen Huang,⁶ Kexin Nie,⁶ Wei Bai,⁷ Zhaosheng Hou,⁸ Rupei Tang,⁹ Hangxun Xu,¹⁰ Ying Zhang,¹⁰ Qing Cai,¹¹ Xianzhu Yang,¹² Zhong Lin Wang,^{1,3,5} and Zhou Li^{1,2,3,14,*}

SUMMARY

Biodegradable polymers (BPs), as fundamental materials for implantable biodegradable medical electronic device (IBMED) fabrication, can be used to prepare the encapsulation layer, substrate, and sensing materials of IBMEDs and the triboelectric materials of implantable triboelectric nanogenerators (TENGs) in particular. The basic properties of these materials determine IBMED performance and application. However, few studies have compared the basic properties of a comprehensive range of BPs, especially in terms of their triboelectric performances and related laws. Here, a comprehensive range of 40 kinds of triboelectric BP films were prepared and tested for triboelectric polarities and degradation in a uniform state. Particularly, we developed a triboelectric series based on these BPs and innovatively summarized the regularities and principles of influence of various main- or side-chain chemical groups on the triboelectric polarities of BPs. This study can not only help researchers to gain insight into the underlying mechanisms of triboelectrification of polymers but also provides important guidance for material selection, especially for the selection of triboelectric BPs for TENG-based IBMEDs in regard to basic research and application.

INTRODUCTION

It is of great significance to develop implantable biodegradable medical electronic devices (IBMEDs) composed of biocompatible and biodegradable materials in order to replace traditional implantable medical electronic devices (IMEDs) for human health monitoring and the treatment of serious diseases over a period of time.^{1,2} Compared with traditional IMEDs, IBMEDs have biodegradable characteristics and can be harmlessly chemically degraded or physically disappear over time in the environment of the human body.³ Since they do not require secondary removal surgery, IBMEDs have remarkable potential and significance for greatly reducing patient injury, surgical risks, and medical costs. At present, IBMEDs have gradually become a research focus in the biomedicine field.⁴ In particular, implantable biodegradable triboelectric nanogenerators (TENGs)^{5–7} possessing “self-powered”⁸ and “biodegradable”⁹ performances have further significance for overcoming the defects of traditional IMEDs, such as the requirements of implanted battery power, or an external generator including transcutaneous leads through skins and tissues, and secondary surgery for device removal.^{10,11}

Biodegradable materials, including polymers, semiconductors, metals, etc., are the basic components of IBMEDs. Among these materials, polymers are incorporated in the

PROGRESS AND POTENTIAL

Biodegradable polymers (BPs) are the raw materials for triboelectric layers of biodegradable triboelectric nanogenerators (TENGs). The triboelectric series can not only help researchers gain insight into the underlying mechanisms of triboelectrification but also has great guiding significance for the selection of triboelectric materials with large serial differences to improve the output of TENGs. However, there are few reports on a triboelectric series comprising a comprehensive range of BPs, and there is also a lack of principles of influence on triboelectric polarities of various BPs. Here, we developed a triboelectric series based on 40 kinds of BPs and innovatively summarized the regularities and principles of influence of various main- or side-chain chemical groups on the triboelectric polarities of BPs. In the research and application of the triboelectricity field, according to this study, researchers can more reasonably select or design triboelectric polymers to control their triboelectric polarities so that the effect of triboelectricity can be enhanced or weakened more controllably.

largest proportion and have the most varied performances and types in devices.¹² Polymers can be prepared for the triboelectric layers of TENGs,⁹ encapsulants,¹³ substrates,¹⁴ sensing materials,¹⁵ and so on. However, few studies have compared a comprehensive range of biodegradable polymers (BPs) in terms of their basic performances, especially with regard to their triboelectric polarities and related laws.^{5,6,9} In this work, 40 kinds of triboelectric BP films covering comprehensive categories were prepared (Figure 1). We researched their preparation methods, degradation *in vitro*, and triboelectric polarities in uniform state and ranked or classified them based on their performances. In particular, we developed a triboelectric series^{16,17} of these BPs in 5 groups (including the 1st group of cellulose and derivatives, the 2nd group of polysaccharides, the 3rd group of proteins and other natural biodegradable polymers [NBPs], the 4th group of poly(α -esters) and poly(α -carbonates), and the 5th group of polyether and other synthetic biodegradable polymers [SBPs]) by ordering the triboelectric polarities of different BPs according to the transferred charge results and innovatively summarized and analyzed the regularities and principles of influence of various main- or side-chain chemical groups on the triboelectric polarity^{18,19} of BPs. Furthermore, we fabricated implantable TENGs using preferred triboelectric BPs and then studied their self-power energy conversion and degradation performance in animals. This study can not only help to further reveal the underlying mechanisms of triboelectrification of polymers but also provides important guidance for material selection for IBMEDs, especially for the selection of triboelectric BPs for TENG-based IBMEDs.

RESULTS AND DISCUSSION

Classification of triboelectric BPs

It is challenging to select suitable BPs for the preparation of IBMEDs with specific functions. The polymers should be biocompatible, biodegradable,²⁰ flexible, and mechanically compatible with the tissue at the implant position.²¹ Some IBMEDs have specific requirements for polymers in terms of electricity, heat, or light performance.^{22,23} BPs can be divided into 2 types based on their origin: NBPs and SBPs.^{24–27} NBPs are mainly created by living organisms, as opposed to SBPs, which are man-made. However, the delineation between the two types is not always clear-cut because some BPs can be obtained both biologically and chemically. According to their sources and chemical structures, NBPs can be further classified into polysaccharides, proteins and poly(amino acids), polynucleotides, and polyhydroxyalkanoates (Figure 2A). Specifically, polysaccharides include cellulose (microcrystalline cellulose [MCC] and bacterial cellulose [BC]) and cellulose derivatives (including methyl cellulose [MC], ethyl cellulose [EC], carboxymethyl cellulose [CMC], hydroxyethyl cellulose [HEC], and hydroxypropyl cellulose [HPC]), starch, alginate, chitin, chitosan, chondroitin sulfate (CS), pullulan, and hyaluronic acid (HA). Proteins include zein, fish collagen, fish gelatin, pig gelatin, silk fibroin (SF), and silk-elastin-like protein (SELP). DNA sodium salt (sodium DNA) from calf thymus is selected as polynucleotide. Poly(amino acids) includes poly- γ -glutamic acid (PGA) and ϵ -polylysine. Poly(3-hydroxybutyrate-copolymer-3-hydroxyhexanoate) (PHBHx) is selected as polyhydroxyalkanoate. SBPs can be divided into poly(α -esters), poly(ortho ester urethanes) (POEUs) (Figure S1), polyanhydrides (Figure S2), polyurethanes (PUs) (Figure S3), polyphosphazenes (Figure S4), polyethylene oxide (PEO), polyvinyl alcohol (PVA), and polyvinyl pyrrolidone (PVP) (Figure 2B). Among them, poly(α -esters) are the most extensively investigated biomedical polymers and include poly(lactic acid-co-glycolic acid) (PLGA); poly(lactic acid) (PLA) and poly(L-lactic acid) (PLLA); poly(ϵ -caprolactone) (PCL); polydioxanone (PDO); poly(butylene succinate); poly(butylene adipate terephthalate) (PBAT); poly(*y*propyl carbonate) (PPC); and poly(trimethylene carbonate) (PTMC). PPC and PTMC can also be categorized as poly(α -carbonates). Each NBP and SBP is described in detail in Note S1.

¹Beijing Institute of Nanoenergy and Nanosystems, Chinese Academy of Sciences, Beijing 101400, China

²School of Physical Science and Technology, Guangxi University, Nanning 530004, China

³School of Nanoscience and Technology, University of Chinese Academy of Sciences, Beijing 100049, China

⁴Key Laboratory of Biomechanics and Mechanobiology, Ministry of Education, Beijing Advanced Innovation Center for Biomedical Engineering, School of Engineering Medicine, Beihang University, Beijing 100191, China

⁵School of Materials Science and Engineering, Georgia Institute of Technology, Atlanta, GA 30332-0245, USA

⁶The Zhejiang University–University of Edinburgh Institute, Zhejiang University, Hangzhou 310058, China

⁷Chengdu Institute of Organic Chemistry, Chinese Academy of Sciences, Chengdu 610041, China

⁸College of Chemistry, Chemical Engineering and Materials Science, Shandong Normal University, Jinan 250014, China

⁹School of Life Sciences, Anhui University, Hefei 230601, China

¹⁰Department of Polymer Science and Engineering, University of Science and Technology of China, Hefei 230026, China

¹¹Beijing University of Chemical Technology, Beijing 100029, China

¹²School of Biomedical Sciences and Engineering, South China University of Technology, Guangzhou 510006, China

¹³These authors contributed equally

¹⁴Lead contact

*Correspondence: zli@binn.cas.cn

<https://doi.org/10.1016/j.matt.2023.09.017>

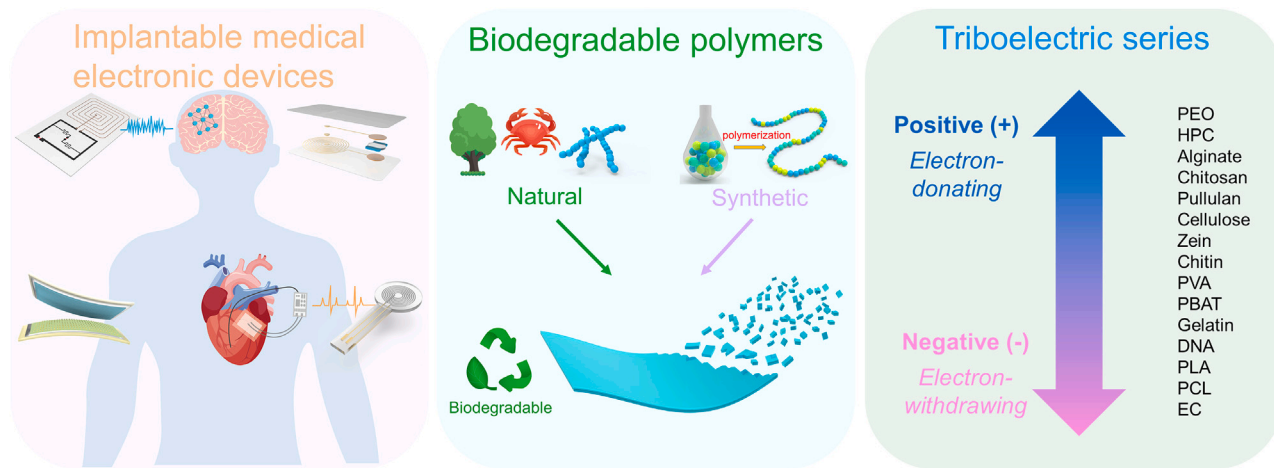


Figure 1. Research on triboelectric BPs in this work

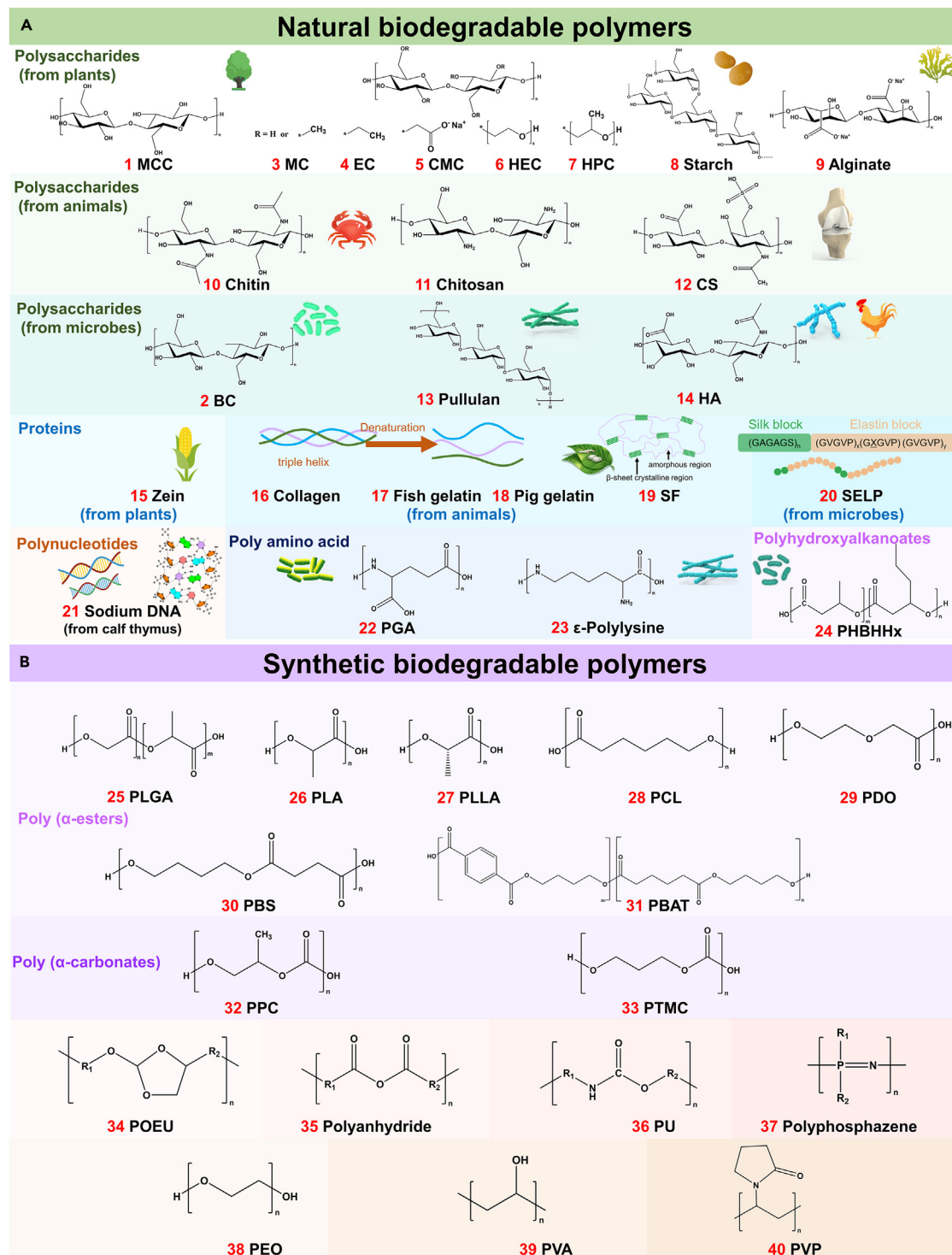
The triboelectric performances and triboelectric series of BP films were mainly studied.

Preparation of BPs films

We used the dissolution-evaporation method to prepare most of the BP films.²⁸ Suitable solvents and dissolution methods were investigated and chosen to dissolve or disperse each NBP (Figure S5A) and SBP (Figure S5B). Some following principles for selecting suitable solvent can be referenced: (1) similar polarity,^{29,30} (2) similar solubility parameter (δ),^{31,32} (3) principle of solvation (available for polar polymers),³³ and (4) the polymer-solvent interaction parameter (χ_{12}) $< 1/2$ principle.^{32,33} Most NBPs can be dissolved in water because of their excellent hydrophilicity and low crystallinity. However, a few NBPs are only soluble in aqueous ethanol, special aqueous solutions, or organic solvents because of their phase-transition temperature, hydrophobicity, or crystallinity of the macromolecules. Most SBPs are hydrophobic and have weak polarity and crystallization, leading to their poor ability to be dissolved in water or ethanol with strong polarity, but they can be well dissolved in dichloromethane or chloroform with a certain polarity. In addition, hexafluoroisopropanol can also dissolve SBPs because hexafluoroisopropanol contains anion radicals that easily interact with the SBPs. In addition, a few SBPs can be well dissolved in water due to their high polarity or abundant hydrophilic groups on main or side chains, which can form hydrogen bonds with water. Suitable solvents for each BP and their dissolution mechanisms are discussed in Note S2. Then, the dissolved BP solutions were poured into Petri dishes, and the solvent was completely evaporated. BP films with flat surfaces were prepared. Most BP films had an integral morphology (Figures S5C and S5D). However, a few BP films were fragmented due to their low molecular weight. Furthermore, the polyanhydride film was prepared by photopolymerization.

Triboelectric polarities of BPs

Determining the contact electrification (CE) or triboelectrification performance¹⁸ and rationalizing the triboelectric series^{16,19} of the BPs were our focus. CE,³⁴ as a common physical phenomenon, refers to the exchange of charges of two materials when they are contacted or rubbed together and then separated. According to CE phenomenon, Zhong Lin Wang et al. invented the TENG in 2012.³⁵ TENGs, based on the coupling of the triboelectrification effect and electrostatic induction, can harvest irregular ambient mechanical energy from the environment and then convert it into electrical power. The main component of TENGs is a pair of triboelectric layer materials, which are often polymer materials.³⁶ Among TENGs, the implantable TENGs based on BPs have "self-powered" and "biodegradable *in vivo*" characteristics^{5,6} and have great significance and potential for solving the application bottleneck of traditional IMEDs and overcoming their



disadvantages, including the requirements of an external generator or implanted battery power, transcutaneous leads through skins and tissues, and secondary surgery for device removal. The rapid development of TENGs^{37,38} has greatly promoted theoretical

research on CE.^{39–41} At present, the charge carriers in the CE process of triboelectric materials may be an electron,⁴² an ion,⁴³ or a small quantity of charged material.⁴⁴ Recently, various experiments have demonstrated that electron transfer due to overlapping electron clouds plays a dominant role in CE of triboelectric materials.^{39,45–47}

The triboelectric series is ranked according to the different triboelectric polarities and triboelectric charge densities (TECDs) of various materials in the CE process.^{18,48,49} The triboelectric series can not only allow researchers to gain insight into the underlying mechanisms of triboelectrification but also has great guiding significance for the selection of triboelectric materials with large serial differences to improve the output of TENGs. Although the first triboelectric series was established more than 260 years ago,⁵⁰ triboelectric materials have been continuously developed.^{16,51–54} However, a triboelectric series is difficult to exactly reproduce by different researchers^{16,55} because it is based on experiments, and the reasons for the resulting differences include diverse experimental methods, experimental conditions^{56,57} (humidity, temperature), or material states^{58–60} (source, roughness, morphology). Moreover, there is not sufficient research on the regularities or principles that cause the distinction in the CE performance of various polymers.¹⁶ Hence, identifying the fundamental principles of influence on the triboelectric polarities of various polymers has become increasingly important. Some recent studies have shown that the chemical groups and the category of a polymer are closely related to its triboelectric polarity and determine its order in triboelectric series.^{18,19}

BPs are the raw materials of the triboelectric layers of implantable biodegradable TENGs. At present, there are few reports on a triboelectric series comprising a comprehensive range of BPs,^{5,6} and there is also a lack of principles of influence on triboelectric polarities of various BPs. Here, 40 kinds of BPs were tested for triboelectric series to further discover or verify the influences of main- or side-chain chemical structures or groups on the triboelectric polarities of different BPs.¹⁸ These 40 BPs basically cover all categories of BPs.^{25,26} To ensure the accuracy of the results, we tried our best to maintain uniform experimental conditions when testing triboelectric polarities, preparation process of the BPs films and films state, including relative humidity (RH: 30% ± 3%), temperature (T: 27°C ± 2°C), film area (2 × 2 cm), and film thickness (100 ± 10 μm) for testing, and each BP film was prepared by dissolving or dispersing 0.5 g polymer in 30 mL solvent, followed by drying for 48 h after pouring the polymer solution into a glass Petri dish (diameter of 66 mm). To test triboelectric polarity, each of the BP films (2 × 2 cm) were periodically contacted with and separated from a polytetrafluoroethylene (PTFE) film under the drive of a linear motor, and the short-circuit charge (transferred charge) was characterized by a digital oscilloscope and an electrometer (Figure 3A). The bottom surface of each BP film was used as the CE surface because the bottom surfaces of all BP films were relatively smooth and had similar arithmetical mean roughness (R_a) due to the template effect of the glass dish surface (Figure S6). We obtained the triboelectric series by ordering the triboelectric polarities of different BPs according to the transferred charge results.

According to the categories and chemical structures of BPs, we divided the 40 BPs into five groups (including the 1st group of cellulose and derivatives, the 2nd group of other polysaccharides, the 3rd group of proteins and other NBP, the 4th group of poly(α-esters) and poly(α-carbonates), and the 5th group of polyether and other SBPs) and then compared their triboelectrification performances (Figures 3B–3G and S7) to better understand the influences of the main- or side-chain functional groups and material categories on the triboelectric polarities of BPs (Figure 5). Detailed discussions of triboelectric series and related principles are summarized below and in Note S3.

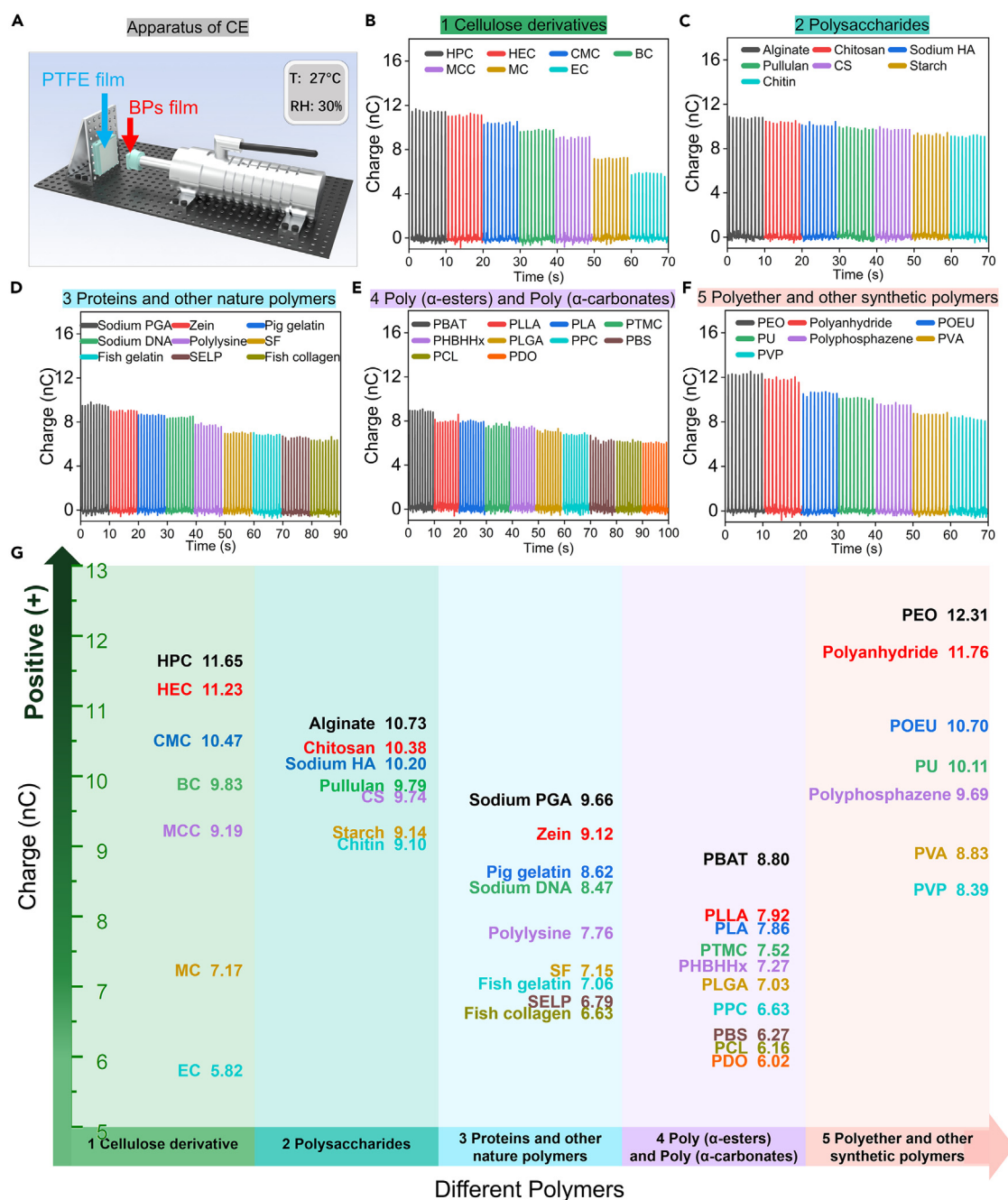


Figure 3. Triboelectric series of 40 kinds of BPs based on the transferred charge of BP films with a PTFE film

(A) Apparatus for testing the transferred charge using the periodical contact-separation method.

(B-F) Ranking of the transferred charges of 5 subgroups (including the 1st group of cellulose and derivatives, the 2nd group of polysaccharides, the 3rd group of proteins and other NBPs, the 4th group of poly(α-esters) and poly(α-carbonates), and the 5th group of polyether and other SBPs).

(G) Triboelectric series of 40 BPs in 5 groups based on the transferred charge results.

(1) The main-chain chemical groups play a major role in determining the position of most BPs in the triboelectric series. The average transferred charge values (mean \pm standard deviation) of different types of BPs (including polyether, polysaccharides, proteins, and poly(α-esters)) are 12.31 ± 0.96 , 9.63 ± 1.59 , 7.75 ± 1.05 , and 7.02 ± 0.71 nC, respectively (the selected BPs are seen in Note S3). For most BPs, the order

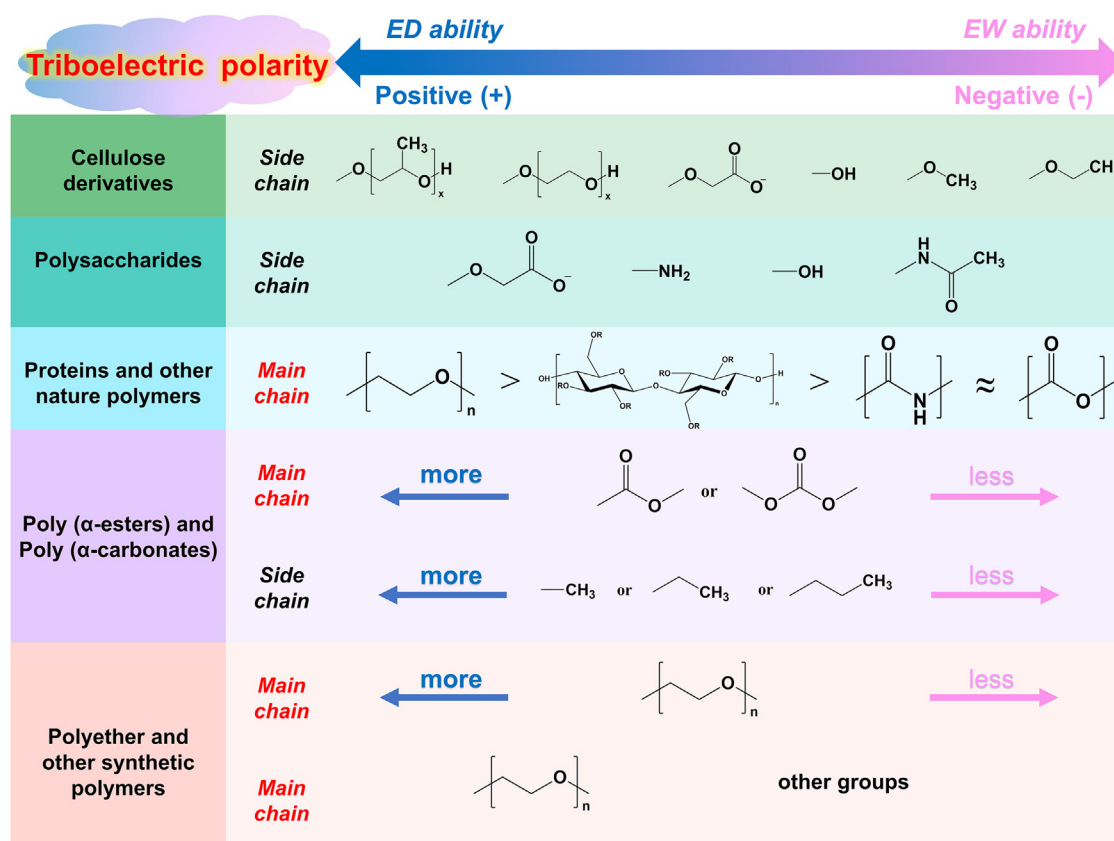


Figure 4. Influences of main- or side-chain chemical groups on triboelectric polarities of different BPs

The regularities and principles of influence in the same group or among groups are shown.

of the BPs in the triboelectric series (from positive to negative) is polyether (with ether bonds), polysaccharides (with glycosidic bonds), proteins or poly(amino acids) (with amide bonds), and poly(α-esters) (with ester bonds or carbonate ester bonds). Among them, the triboelectric polarities of most proteins and poly(α-esters) are similar (Figures 3G and 4). To better evaluate the degree of triboelectric positive polarity of different main-chain groups, we use the PEO (with main-chain ether bonds) with the most positive polarity as the reference and set the degree of positive polarity of PEO ($Q_{PEO} = 12.31 \text{ nC}$) to 100% ($P_{PEO} = 100\%$). The degree of positive polarity of different main chains can be calculated according to the formula

$$P_j = \frac{\overline{Q}_j}{Q_{PEO}} \quad (\text{Equation 1})$$

where P_j is the degree of positive polarity of the different main chains, \overline{Q}_j is the mean transferred charge value of all BPs with similar main chains, and Q_{PEO} ($Q_{PEO} = 12.31 \text{ nC}$) is the transferred charge value of PEO. Therefore, the degrees of positive polarity of polyether (with ether bonds), polysaccharides (with glycosidic bonds), proteins (with amide bonds), and poly(α-esters) (with ester bonds or carbonate ester bonds) are 100%, 78.22%, 62.96%, and 57.03%, respectively.

(2) The side-chain chemical groups affect the triboelectric polarities of BPs. Most BPs with similar main chains but different side chains (excluding side groups with strong polarity) tend to have different but close orderings in the triboelectric series (Figure 3G). We investigate the degree of influence of side- or main-chain groups on

the triboelectric polarities of BPs by the standard deviation of the transferred charge value. The formula of standard deviation is given as

$$\sigma = \sqrt{\frac{\sum_{i=1}^n (Q_i - \bar{Q})^2}{n}} \quad (\text{Equation 2})$$

where σ is the standard deviation of the transferred charge values, Q_i is the transferred charge value of each BP with similar main-chains, \bar{Q} is the mean transferred charge value of all BPs with similar main-chains, and n is the total number of the BPs. In statistics, the standard deviation can quantify the dispersion or variation of a set of values, so the larger the standard deviation, the greater the influence of functional groups on the triboelectric polarities. Firstly, we research the degree of influence of different side-chain groups. The average transferred charge values (mean \pm standard deviation) of different types of BPs (including most polysaccharides, proteins, poly(α -esters), and polyether) are 9.63 ± 1.59 , 7.75 ± 1.05 , 7.02 ± 0.71 , and 12.31 ± 0 nC, respectively (the selected BPs are seen in Note S3). Secondly, we investigate the degree of influence of different main-chain groups by further calculating the average value (9.18 ± 2.36 nC) of above average transferred charge values. For BPs with similar main chains but different side chains, the standard deviations of transferred charge values are mostly less than 1.6 nC. In contrast, for BPs with different main chains, the standard deviation is greater than 2.3 nC. By comparison, we can see that the degree of influence of most side-chain groups on the triboelectric polarities of BPs is smaller than that of the main-chain groups.

The 1st group includes cellulose and cellulose derivatives, and the order of these BPs in the triboelectric series (from positive to negative) is HPC,⁶¹ HEC,⁶² CMC,⁶³ BC,⁶⁴ MCC,⁶⁵ MC,⁶⁶ and EC⁶⁷ (Figures 3B and S7A). For the 1st group, we infer that the strength of the electron-donating (ED) ability of the side groups follows the order [-OCH₂CH(CH₃)O-]_n > [-OCH₂CH₂O-]_n > -OCH₂COO⁻ > -OH > -OCH₃ > -OCH₂CH₃ (Figure 4). Cellulose is a chain polymer linked by anhydro-D-glucose repeating units through β (1-4) glycosidic bonds. Cellulose and cellulose derivatives have the same main chain but different side groups. The hydroxyl groups (-OH) at the C-2, C-3, or C-6 position of repeating anhydro-D-glucose units are partially converted into [-OCH₂CH(CH₃)O-]_n, [-OCH₂CH₂O-]_n, -OCH₂COO⁻Na⁺, -OCH₃, or -OCH₂CH₃ groups, respectively, forming different cellulose ethers. Different functional groups have different ED or electron-withdrawing (EW) abilities.⁶⁸ Some studies have shown that polymers possessing polyether groups ([-CH₂CH₂O-]_n) have greater ED abilities during CE and show excellent positive polarity in triboelectric series, even higher than that of the common tribo-positive material polyamide.^{69,70} In this group, the side chains of HPC and HEC contain abundant polyether groups, resulting in HPC and HEC being at the most positive positions in the triboelectric series among cellulose derivatives. By comparing these two BPs, it can be seen that the methyl group (-CH₃) in the hydroxypropyl group has a greater ED ability than the hydrogen in the hydroxyethyl group,¹⁸ and thus the HPC film appears to be more positive than the HEC film; CMC contains abundant negatively charged carboxylate (-COO⁻) side groups, so the CMC film exhibits a better ED ability during the contact-separation process, resulting in a relatively positive polarity in the triboelectric series.⁶³ BC and MCC contain a large number of hydroxyl (-OH) side groups, and the ED ability of the -OH group is weaker¹⁸ than that of the -COO⁻ group, so BC and MCC exhibit more negative polarity than CMC. In comparison, the BC film has more ultrafine nanofibrils and more microstructure⁶⁴ on the surface than the MCC film, resulting in a slightly higher positive polarity. In addition, the reason why MCC exhibits less ED ability than BC may be that a small number of functional groups are introduced into the MCC molecules during its hydrolysis preparation. In addition, the order of these BPs in the triboelectric series (from positive to

negative) is cellulose (including BC and MCC), MC, and EC, which is consistent with the order of the EW inductive effect of the groups (-OCH₂CH₃) > -OCH₃) > -OH).⁶⁶ It should be noted that in the 1st group, the degree of substitution (DS) of different cellulose derivatives varies because it is difficult to purchase these cellulose derivatives with the same DS, but the DSs of these different cellulose derivatives range from 0.9 to 1.4. If the DS is consistent, better triboelectric polarities results can be obtained.

The 2nd group includes polysaccharides, and the order of the BPs in this group in triboelectric series (from positive to negative) is alginate,⁷¹ chitosan,^{72,73} sodium HA,⁷⁴ pullulan,⁷⁵ CS, starch,⁷⁶ and chitin⁷⁷ (Figures 3C and S7B). For this group, we infer that the strength of the ED ability of the side groups follows the order of carboxylate group > amino group > hydroxyls group > N-acetyl amide group (Figure 4). Polysaccharides in the 2nd group are polymers made of different monosaccharides (hexose) or oligosaccharides or corresponding derivative units, and their main-chain structures are very similar. Thus, these polysaccharides have different triboelectric polarities and ED or EW abilities due to their different side groups. Each repeating unit of alginate contains one -COO⁻ group and two -OH groups, and the -COO⁻ group exhibits a better ED ability in CE,⁶³ so alginate has the most positive polarity in the triboelectric series among BPs of the 2nd group. Moreover, the positive polarity of alginate is higher than that of CMC in the 1st group because the amount of carboxylate groups in the CMC unit is less than that of alginate, and each unit of CMC contains less than one -CH₂COO⁻ substituent (due to the DS of carboxymethyl groups being approximately 0.7–0.9 for the CMC used in this work). Each repeating unit of chitosan contains an amino group (-NH₂) and two -OH groups, and the amino group also exhibits a better ED ability⁶⁸ due to its tendency to lose electrons, becoming positively charged during the CE process, so chitosan also possesses a good positive polarity following the alginate.⁶³ Each repeating unit of chitin contains one N-acetyl amide group and two hydroxyl groups. The N-acetyl amide group has an obviously weaker ED ability than the carboxylate group, so chitin is more negative than alginate and is located at the end of the triboelectric series with regard to the BPs in the 2nd group. Pullulan and starch only contain hydroxyl groups as side groups, and the ED ability of the hydroxyl group¹⁸ is between that of the carboxylate group and the N-acetyl amide group. As a result, the triboelectric positive polarities of pullulan and starch are between that of alginate and chitin. Sodium HA and CS are composed of disaccharide repeating units. Each repeating unit of sodium HA contains a carboxylate group, an N-acetyl amide group, and four hydroxyl groups. Each repeating unit of CS contains a carboxylate group, a sulfate group, one N-acetyl amide group, and three hydroxyl groups. The triboelectric positive polarities of sodium HA and CS are also between those of alginate and chitin. Specifically, the triboelectric polarity of sodium HA is more positive than that of polysaccharides (such as pullulan, starch, or cellulose) containing only hydroxyl side groups due to the strong ED ability of the carboxylate group in sodium HA. Furthermore, although the glycosidic bond of polysaccharides and derivatives in the 1st group and the 2nd group is a kind of ether bond, due to the structural particularity of the polysaccharides, we discuss the glycosidic bond separately. At the same time, we found that the density of oxygen atoms in the polysaccharide main chain is lower than that of PEO (with repeating -CH₂-CH₂-O- groups in the main chain), resulting in a weaker positive polarity of polysaccharides than that of PEO.

The 3rd group includes protein, poly(amino acids), and DNA, and the order in triboelectric series (from positive to negative) is sodium PGA, zein,⁷⁸ pig gelatin, sodium DNA,⁷⁹ polylysine,⁸⁰ SF,⁸¹ fish gelatin,⁸² SELP, and fish collagen⁸³ (Figures 3D and

S7C). For the 3rd group, we find that sodium PGA has the largest positive polarity, most likely due to its highest density of carboxylate side groups compared with that of other proteins, as the carboxylate group is considered to have a strong ED ability. In addition, the triboelectric polarities of different proteins may be related to the type and proportion of amino acids,⁷⁸ and it is necessary to study a triboelectric series of different amino acids in future work. Moreover, the triboelectric polarities of most proteins (rich in amide bonds in the main chain) are close to that of poly(α -esters) in the 4th group but are more negative than that of polyether in the 5th group and most polysaccharides (including derivatives) in the 1st group and the 2nd group, so it is inferred that the ED abilities of the main-chain ester bond⁸⁴ and amide bonds⁷⁰ are weaker than that of the main-chain ether bonds of polyether (such as PEO) and the glycosidic bonds of polysaccharides (Figure 4).

(3) The triboelectric polarities are related to the density of the functional groups in the main chain or the side chain. The higher the density of ester bonds or ether bonds in the main chain, the stronger the triboelectric positive polarity of the poly(α -esters) or polyether. More side-chain alkanes also tend to increase the positive polarity of the poly(α -esters) (Figures 3G and 4).

The 4th group includes poly(α -esters) (including poly(α -carbonates)), and the order in the triboelectric series (from positive to negative) is PBAT, PLLA, PLA, PTMC, PHBHHx, PLGA,⁵ PPC,⁸⁵ PBS,⁸⁶ PCL,^{5,84,86} and PDO (Figures 3E and S7D). Except for that of PBAT, the main chains of these polymers are mainly composed of repeating units of alkanes and esters or carbonate, and some have alkane side groups. For the 4th group, we made three inferences. First, the ED ability and positive polarity of poly(α -esters) increase with increasing density of the main-chain ester (or carbonate ester) bonds (Figure 4).^{5,84,86} We used the number of carbon atoms between adjacent main-chain ester (or carbonate ester) bonds (excluding the side chain) to reflect the ester bond density, i.e., the lower the number of carbon atoms, the higher the ester bond density. The order of the positive polarity (from positive to negative) of poly(α -esters) has the following relationship with the number of carbon atoms: PLLA or PLA (2, where 2 means there are 2 carbon atoms between adjacent ester bonds) > PHBHHx (3) > PBS (4) > PCL (6). Second, for poly(α -esters) with the same (or similar) density of main-chain ester (or carbonate ester) bonds, a higher density of side-chain alkane (-CH₃, -CH₂CH₃, or -CH₂CH₂CH₃) correlated with a more positive polarity (Figure 4).¹⁸ The corresponding ordering is PLA > PLGA, PHBHHx > PLGA, PHBHHx > PPC. Third, PBAT with benzene rings in its main chain has the most positive polarity among the BPs in the 4th group.

(4) Repeating ether groups were verified to have the highest triboelectric positive polarity in BPs. PEO (with abundant main-chain [-CH₂-CH₂-O-]_n groups) was verified to have the highest triboelectric positive polarity among all BPs (1st–5th groups). HPC or HEC (with abundant side-chain [-OCH₂CH(CH₃)O-]_n or [-OCH₂CH₂O-]_n groups) has the highest positive polarities among all polysaccharides and derivatives (Figure 3G).

The 5th group includes polyether and other SBPs, and the order of the BPs in the triboelectric series (from positive to negative) is PEO, polyanhydride, POEU, PU, polyphosphazene, PVA, and PVP (Figures 3F and S7E). Among them, PEO, polyanhydride,⁸⁷ POEU,⁸⁸ and PU⁸⁹ have a certain proportion of main-chain [-CH₂-CH₂-O-]_n groups (ether bonds). For the 5th group, we made two inferences. First, the ED ability and positive polarity of the BPs increase with increasing the mass ratio of main-chain [-CH₂-CH₂-O-]_n groups (Figure 4). The order of the positive polarity

(from positive to negative) of these BPs has the following relationship with the mass ratio of main-chain $[-\text{CH}_2-\text{CH}_2-\text{O}-]_n$ groups (including repeating ortho ester groups): PEO (100 wt %, where 100 wt % means that the mass of main-chain $[-\text{CH}_2-\text{CH}_2-\text{O}-]_n$ groups accounts for 100 wt % of the main-chain mass) > POEU (45.9 wt %) > PU (37.8 wt %). It should be noted that POEU contains repeating ortho ester groups,⁸⁸ and its structure and triboelectric polarity are considered to be similar to $[-\text{CH}_2-\text{CH}_2-\text{O}-]_n$, so the mass ratio of ortho ester groups is also included. Polyanhydride has a lower mass ratio of main-chain $[-\text{CH}_2-\text{CH}_2-\text{O}-]_n$ (16.9 wt %), but the reason why it shows improved transferred charge is that the adhesion performance and the adhesion energy of polyanhydride film with PTFE increase the intensity of triboelectrification during CE. Second, the contribution of $[-\text{CH}_2-\text{CH}_2-\text{O}-]_n$ groups to the ED ability and positive polarity of these BPs is higher than that of other chemical groups (Figure 4).^{69,70,84} Among all BPs (1st–5th groups), PEO (with abundant main-chain $[-\text{CH}_2-\text{CH}_2-\text{O}-]_n$ groups) was verified to have the highest triboelectric positive polarity (Figure 3G).

(5) The triboelectrification effects of BP films with adhesion performance or fragmented morphology can be enhanced or reduced, respectively.

Furthermore, some factors that affected the transferred charge during CE for a few BPs were identified, which caused some errors in their triboelectric polarities and triboelectric series ranking results. Specifically, we found that BP films with adhesion performance (such as the PTMC and polyanhydride films) showed an improved transferred charge during CE with PTFE membranes because the adhesion energy⁹⁰ increased the intensity of triboelectrification during CE. In contrast, BP films with a fragmented morphology (such as the CS, collagen, and PDO films) showed a reduced transferred charge during CE with PTFE membranes.⁹¹ However, the polylysine film, composed of 50 wt % ϵ -polylysine and 50 wt % α -polylysine, which has both a fragmented morphology due to the low molecular weight of ϵ -polylysine and adhesion performance because of α -polylysine being used as bioadhesive, was found to have a certain error in transferred charge and triboelectric series ranking. In addition, the starch composite film contained 15 wt % glycerol, which had a certain impact on its triboelectric polarity.

Degradation performance

The biodegradation of these polymers involves the cleavage of enzymatically or hydrolytically sensitive bonds, leading to polymer erosion.²⁴ According to their degradation mechanism, BPs can be further divided into enzymatically degradable BPs and hydrolytically degradable BPs. Most NBP are easily degraded by enzymes in the human body.^{20,92} In comparison, most SBPs are biologically inert, and their degradation mechanism is mainly hydrolysis, but enzymes in the human body may also participate in the degradation of SBPs to a certain extent.^{93,94} In addition, reactive oxygen or nitrogen species released from inflammatory cells can also accelerate the degradation of BPs by oxidation.²⁰ In terms of device degradation, IBMEDs can be considered to be degradable as long as they are physically damaged in the physiological environment.⁹⁵ Most NBPs are water-soluble polymers, and most SBPs are hydrolytically BPs.²⁶ Therefore, we used phosphate-buffered saline at 37°C to simulate human body fluid and investigated the degradation performance of different BP films in phosphate-buffered saline. According to their degradation time, i.e., the point when the BP films' morphology changes significantly or the mass decreases significantly, the 40 BPs can be divided into 6 types as follows: rapid dissolving (the 1st type); rapid swelling (the 2nd type); short-term degradable (the 3rd type); medium-term degradable (the 4th type); long-term degradable (the 5th type); and longer-term degradable (the 6th type). The

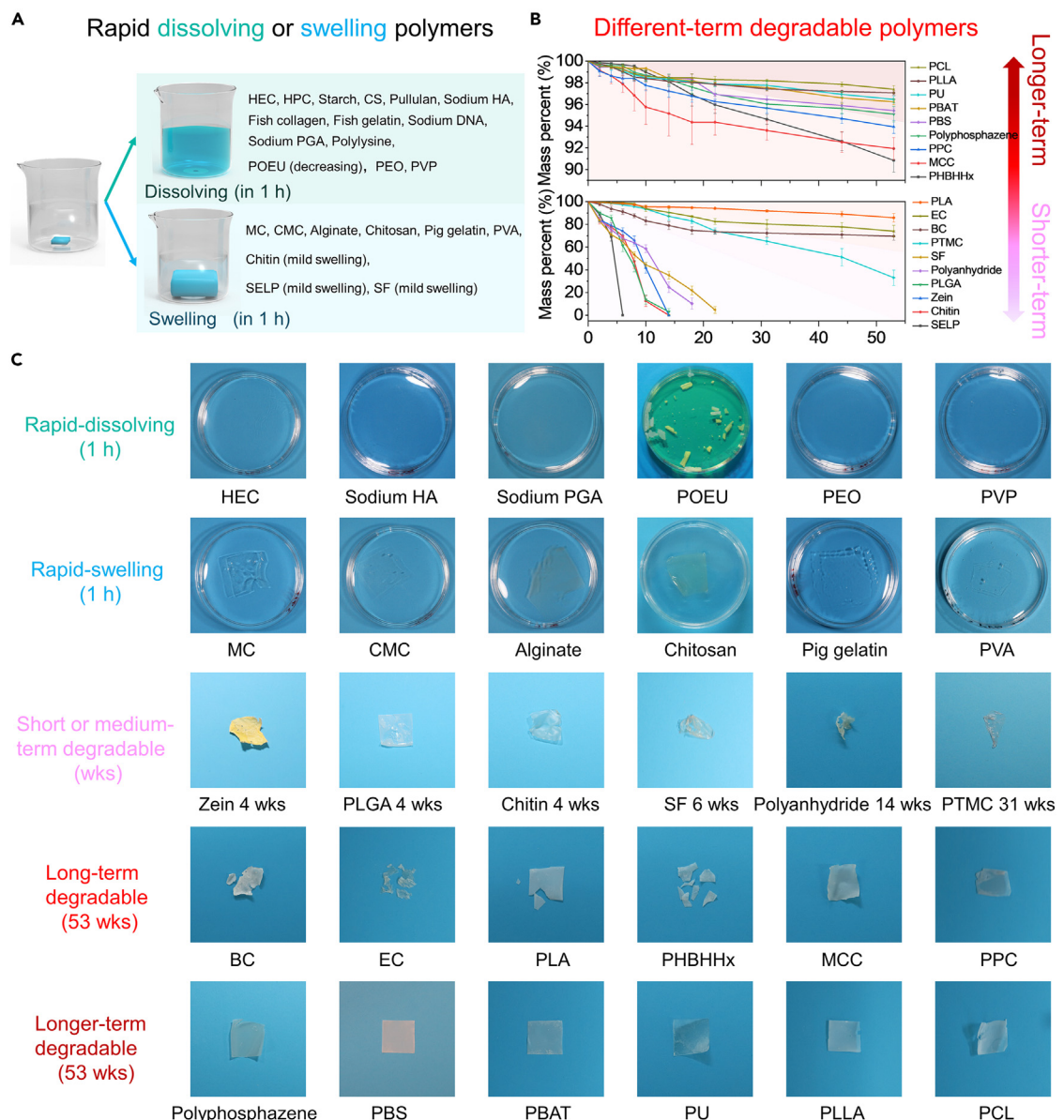


Figure 5. Degradation performance *in vitro* of the 40 kinds of BPs

Forty kinds of BP films with a size of 2×2 cm were soaked in a polystyrene Petri dish containing phosphate-buffered saline, respectively. The degradation process and performance of the BPs in phosphate-buffered saline were studied.

(A) Classification of rapidly dissolving or swelling polymers.

(B) Classification of different-term degradable polymers and mass variation of different-term degradable polymers in phosphate-buffered saline. ($n = 3$ independent samples. Data are presented as mean \pm standard deviation.)

(C) The 6 types of BPs (including rapid dissolving, rapid swelling, short-term degradable, medium-term degradable, long-term degradable, and longer-term degradable) divided according to their degradation time when the BP film morphology changes significantly or the mass decreases significantly. Several BPs for each type are listed, and the morphology changes of the BP films at corresponding degradation times are shown.

degradation performance of each BP film among the 6 types, as well as their degradation mechanisms, are discussed in Note S4 and shown in Figure 5.

Conclusions

In conclusion, the basic performances of a comprehensive range of triboelectric BPs for IBMEDs were studied. Particularly, we innovatively summarized the regularities

and principles of influence of various main- or side-chain chemical groups on the triboelectric polarities of BPs and developed a triboelectric series based on these BPs. The regularities and principles included that (1) the main-chain chemical groups play a major role in determining the position of most BPs in the triboelectric series; (2) the side-chain chemical groups affect the triboelectric polarities of BPs; (3) the triboelectric polarities are related to the density of the functional groups in the main chain or the side chain; (4) repeating ether groups was verified to have the highest triboelectric positive polarity in BPs; and (5) the triboelectrification effects of BP films with adhesion performance or fragmented morphology can be enhanced or reduced, respectively. The significance of this study includes further revealing the underlying mechanisms of triboelectrification of polymers and providing guidance for material selection for IBMEDs, especially for the selection of triboelectric BPs for TENG-based IBMEDs.

EXPERIMENTAL PROCEDURES

Resource availability

Lead contact

Further information and requests for resources and reagents should be directed to and will be fulfilled by the lead contact, Zhou Li (zli@binn.cas.cn).

Materials availability

This study did not generate new unique reagents. All relevant vendors and preparation procedures are included in the [supplemental information](#).

Data and code availability

Any additional information required to reanalyze the data reported in this paper is available from the lead contact upon request.

Materials

Details of BPs and other reagents are listed in [Tables S1–S3](#).

Preparation of BP films

We used the dissolution-evaporation method to prepare most of the BP films. At a certain temperature (most BPs in this work were dissolved at room temperature), 0.5 g polymer powders or particles were dissolved or completely dispersed in 30 mL of a suitable solvent, such as water, ethanol, methylene chloride, chloroform, hexafluoroisopropanol, etc. Then, the solutions were poured into glass Petri dishes (diameter of 66 mm) and dried in an air oven at 40°C (for polymers dissolved in water) for 48 h or at room temperature (for polymers dissolved in organic solvents) for 48 h until completely dry polymer films were formed (thickness of $100 \pm 10 \mu\text{m}$). The films were cut into $2 \times 2 \text{ cm}$ samples for degradation and triboelectric performance experiments.

In addition, the preparation of a few of BP films required more processes or other methods. For example, starch (amylose) was first prepared as a paste under high temperature and pressure and then was mixed with glycerol and dried on a plate; the chitosan film needed to be further cleaned to remove acetic acid; and the poly-anhydride film was prepared by photopolymerization. The detailed methods are listed in [Note S2](#).

Degradation *in vitro*

Each BP film with a size of $2 \times 2 \text{ cm}$ (initial mass: m_1) was soaked in a polystyrene Petri dish containing phosphate-buffered saline. Then, the Petri dish was placed in a

constant temperature (37°C) incubator, and the phosphate-buffered saline solution was replaced every 2 weeks. After the polymer film was washed with distilled water and then dried at 37°C to a constant weight, the residual mass (m_2) of the polymer film was obtained by weighing. The residual mass ratio of the polymer film at different degradation times was calculated by the following formula: residual mass ratio = m_2/m_1 .

Triboelectric polarities of BPs

All tested BP films ($2 \times 2 \text{ cm}$) were cleaned with flowing nitrogen gas and were kept in sealable bag. The aluminum tapes were attached to the BP films as the electrode layer. The temperature ($27^{\circ}\text{C} \pm 2^{\circ}\text{C}$) and humidity ($30\% \pm 3\%$) for each triboelectric test were maintained. Due to its good electronegativity, a PTFE film ($4 \times 4 \text{ cm}$, thickness of $100 \mu\text{m}$) was selected as the same counterpart material to contact different BPs. First, the tested BP films ($2 \times 2 \text{ cm}$) with electrode layers were fixed on an acrylic substrate ($2 \times 2 \text{ cm}$) by 3M double-coated urethane foam tape with the electrode facing toward the surface of the acrylic substrate. The PTFE film with an aluminum electrode layer was also fixed on another acrylic substrate ($4 \times 4 \text{ cm}$). Then, the BP films (bottom surface) were periodically contacted with and separated from the PTFE film, respectively, under the drive of a linear motor (LinMot). A digital oscilloscope (Teledyne LeCroy, HDO6104) and an electrometer (Keithley, 6517B) were employed to characterize the short-circuit charge. All data were tested at least 3 times. Long-cycle tests for triboelectric polarities of selected BP films were also conducted, and the results are shown in [Figures S8A–S8D](#).

Fabrication and electrical measurement of TENGs based on BPs

First, the back surfaces of the PEO and EC films were deposited with magnesium as electrode layers (100 nm) by Magnetron Sputter (635, Denton Discovery), respectively. Then, these two films ($2 \times 2 \text{ cm}$) were assembled with spacers, and two lead wires were, respectively, connected to two electrode layers. Finally, the SF, PTMC, and PCL films were employed as encapsulation layers for packaging the device, respectively. The edges of the encapsulation layers were encapsulated with adhesive or with heat-sealing technology. A digital oscilloscope (Teledyne LeCroy, HDO6104) and an electrometer (Keithley, 6517B) were employed to characterize the open-circuit voltage (V_{oc}), the short-circuit current (I_{sc}), and the short-circuit transferred charge (Q_{sc}) of the TENG when a linear motor exerted a periodic force on the TENG. The results are discussed in [Notes S5](#) and [S6](#) and shown in [Figures S8E](#), [S8F](#), and [S9A–S9D](#).

In vivo test of TENG

Sprague Dawley (SD) rats (male, 150–200 g) were purchased from Charles River Laboratories (Beijing, China). Before the implantation, TENGs were sterilized by ultraviolet light. Then, isoflurane gas was used to pre-anesthetize the rats. Next, sodium pentobarbital (1%) was employed for intraperitoneal injection (40 mg kg^{-1}) to maintain anesthesia. Then, the abdominal subcutaneous skin of each SD rat was incised to implant the TENG. Periodic slight pressure from a finger ([Figures S10A](#) and [S10B](#)) was applied on the skin of the implantation region to drive the TENG. V_{oc} , I_{sc} , and Q_{sc} were measured by a digital oscilloscope (Teledyne LeCroy, HDO6104) and an electrometer (Keithley, 6517B). All experimental procedures were reviewed and approved by the Committee on Ethics of the Beijing Institute of Nanoenergy and Nanosystems. The results are discussed in [Notes S6](#) and [S7](#) and shown in [Figures S9E–S9I](#).

SUPPLEMENTAL INFORMATION

Supplemental information can be found online at <https://doi.org/10.1016/j.matt.2023.09.017>.

ACKNOWLEDGMENTS

This work was supported by the National Key Research and Development Program of China, China (2022YFE0111700 and 2022YFB3804700); the National Natural Science Foundation of China, China (T2125003, 52203325, and 82102231); the Beijing Natural Science Foundation, China (JQ20038 and L212010); and the Fundamental Research Funds for the Central Universities, China (E0EG6802X2). We thank Prof. Linhua Song (China University of Petroleum), Yuanbin Bai (Bluepha Co., Ltd.), Baoshan Li (Zdair Materials Technology Co., Ltd.), and Minglong Yuan (Biochem-ZX Co., Ltd.) for their technical assistance and Dengjie Yu, Li Wu, Lu Wang, Junlin Yuan, Cong Li, Ruizeng Luo, etc., for their assistance in experiments and discussion.

AUTHOR CONTRIBUTIONS

Conceptualization, H.M., Z. Liu, and Z. Li; methodology, H.M., Z. Liu, Q.Y., and Z. Li; investigation, H.M., Q.Y., Z. Liu, J.X., Y.B., X.Q., and Z. Li; validation, H.M., Z. Liu, and Z. Li; formal analysis, H.M., Z. Li, P.T., D.L., and Z.L.W.; resources, Z. Li, H.M., Z. Liu, W.H., K.N. W.B., Z.H., R.T., H.X., Y.Z., Q.C., and X.Y.; writing – original draft, H.M., Z. Liu, Z. Li, and Y.G.; writing – review & editing, H.M. and Z. Li; funding acquisition, Z. Li, H.M., and Z. Liu; supervision, Z. Li and H.M.

DECLARATION OF INTERESTS

The authors declare no competing interests.

Received: July 28, 2023

Revised: September 14, 2023

Accepted: September 27, 2023

Published: October 31, 2023

REFERENCES

1. Hwang, S.-W., Tao, H., Kim, D.-H., Cheng, H., Song, J.-K., Rill, E., Brenckle, M.A., Panilaitis, B., Won, S.M., Kim, Y.-S., et al. (2012). A physically transient form of silicon electronics. *Science* 337, 1640–1644.
2. Choi, Y.S., Yin, R.T., Pfenniger, A., Koo, J., Avila, R., Benjamin Lee, K., Chen, S.W., Lee, G., Li, G., Qiao, Y., et al. (2021). Fully implantable and bioresorbable cardiac pacemakers without leads or batteries. *Nat. Biotechnol.* 39, 1228–1238.
3. La Mattina, A.A., Mariani, S., and Barillaro, G. (2020). Bioresorbable materials on the rise: from electronic components and physical sensors to *in vivo* monitoring systems. *Adv. Sci.* 7, 1902872.
4. Yang, Q., Liu, T.-L., Xue, Y., Wang, H., Xu, Y., Emon, B., Wu, M., Rountree, C., Wei, T., Kandela, I., et al. (2022). Ecoresorbable and bioresorbable microelectromechanical systems. *Nat. Electron.* 5, 526–538.
5. Zheng, Q., Zou, Y., Zhang, Y., Liu, Z., Shi, B., Wang, X., Jin, Y., Ouyang, H., Li, Z., and Wang, Z.L. (2016). Biodegradable triboelectric nanogenerator as a life-time designed implantable power source. *Sci. Adv.* 2, e1501478.
6. Jiang, W., Li, H., Liu, Z., Li, Z., Tian, J., Shi, B., Zou, Y., Ouyang, H., Zhao, C., Zhao, L., et al. (2018). Fully bioabsorbable natural-materials-based triboelectric nanogenerators. *Adv. Mater.* 30, 1801895.
7. Ouyang, H., Li, Z., Gu, M., Hu, Y., Xu, L., Jiang, D., Cheng, S., Zou, Y., Deng, Y., Shi, B., et al. (2021). A bioresorbable dynamic pressure sensor for cardiovascular postoperative care. *Adv. Mater.* 33, 2102302.
8. Zheng, Q., Tang, Q., Wang, Z.L., and Li, Z. (2021). Self-powered cardiovascular electronic devices and systems. *Nat. Rev. Cardiol.* 18, 7–21.
9. Chao, S., Ouyang, H., Jiang, D., Fan, Y., and Li, Z. (2021). Triboelectric nanogenerator based on degradable materials. *EcoMat* 3, e12072.
10. Koutentakis, M., Siminelakis, S., Korantzopoulos, P., Petrou, A., Priavali, H., Mpakas, A., Gesouli, H., Apostolakis, E., Tsakiridis, K., Zarogoulidis, P., et al. (2014). Surgical management of cardiac implantable electronic device infections. *J. Thorac. Dis.* 6, S173–S179.
11. Elmistekawy, E. (2019). Safety of temporary pacemaker wires. *Asian Cardiovasc. Thorac. Ann.* 27, 341–346.
12. Han, W.B., Lee, J.H., Shin, J.W., and Hwang, S.W. (2020). Advanced materials and systems for biodegradable, transient electronics. *Adv. Mater.* 32, 2002211.
13. Choi, Y.S., Koo, J., Lee, Y.J., Lee, G., Avila, R., Ying, H., Reeder, J., Hambitzer, L., Im, K., Kim, J., et al. (2020). Biodegradable poly(ether anhydrides) as encapsulation layers for transient electronics. *Adv. Funct. Mater.* 30, 2000941.
14. Zhang, X., and Bellan, L.M. (2017). Composites formed from thermoresponsive polymers and conductive nanowires for transient electronic systems. *ACS Appl. Mater. Interfaces* 9, 21991–21997.
15. Lu, D., Yan, Y., Avila, R., Kandela, I., Stepien, I., Seo, M.H., Bai, W., Yang, Q., Li, C., Haney, C.R., et al. (2020). Bioresorbable, wireless, passive sensors as temporary implants for monitoring regional body temperature. *Adv. Healthcare Mater.* 9, 2000942.

16. Zou, H., Zhang, Y., Guo, L., Wang, P., He, X., Dai, G., Zheng, H., Chen, C., Wang, A.C., Xu, C., and Wang, Z.L. (2019). Quantifying the triboelectric series. *Nat. Commun.* 10, 1427–1429.
17. Liu, D., Zhou, L., Cui, S., Gao, Y., Li, S., Zhao, Z., Yi, Z., Zou, H., Fan, Y., Wang, J., and Wang, Z.L. (2022). Standardized measurement of dielectric materials' intrinsic triboelectric charge density through the suppression of air breakdown. *Nat. Commun.* 13, 6019–6110.
18. Li, S., Nie, J., Shi, Y., Tao, X., Wang, F., Tian, J., Lin, S., Chen, X., and Wang, Z.L. (2020). Contributions of different functional groups to contact electrification of polymers. *Adv. Mater.* 32, 2001307.
19. Zhang, X., Chen, L., Jiang, Y., Lim, W., and Soh, S. (2019). Rationalizing the triboelectric series of polymers. *Chem. Mater.* 31, 1473–1478.
20. Li, Z.Q., Li, C.H., Fitzpatrick, V., Ibrahim, A., Zwierstra, M.J., Hanna, P., Lechtig, A., Nazarian, A., Lin, S.J., and Kaplan, D.L. (2020). Design of biodegradable, implantable devices towards clinical translation. *Mil. Med. Res.* 7, 61–81.
21. Song, E., Li, J., Won, S.M., Bai, W., and Rogers, J.A. (2020). Materials for flexible bioelectronic systems as chronic neural interfaces. *Nat. Mater.* 19, 590–603.
22. Lee, G., Choi, Y.S., Yoon, H.-J., and Rogers, J.A. (2020). Advances in physicochemically stimuliresponsive materials for on-demand transient electronic systems. *Matter* 3, 1031–1052.
23. Won, S.M., Song, E., Reeder, J.T., and Rogers, J.A. (2020). Emerging modalities and implantable technologies for neuromodulation. *Cell* 181, 115–135.
24. Zhang, Z., Ortiz, O., Goyal, R., and Kohn, J. (2014). Biodegradable Polymers. *Handbook of Polymer Applications in Medicine and Medical Devices*, pp. 303–335.
25. Doppalapudi, S., Jain, A., Khan, W., and Domb, A.J. (2014). Biodegradable polymers—an overview. *Polym. Adv. Technol.* 25, 427–435.
26. Nair, L.S., and Laurencin, C.T. (2007). Biodegradable polymers as biomaterials. *Prog. Polym. Sci.* 32, 762–798.
27. Hosseini, E.S., Dervin, S., Ganguly, P., and Dahiya, R. (2021). Biodegradable materials for sustainable health monitoring devices. *ACS Appl. Bio Mater.* 4, 163–194.
28. Yang, F., Li, J., Long, Y., Zhang, Z., Wang, L., Sui, J., Dong, Y., Wang, Y., Taylor, R., Ni, D., et al. (2021). Wafer-scale heterostructured piezoelectric bio-organic thin films. *Science* 373, 337–342.
29. Spange, S., Vilsmeier, E., Fischer, K., Reuter, A., Prause, S., Zimmermann, Y., and Schmidt, C. (2000). Empirical polarity parameters for various macromolecular and related materials. *Macromol. Rapid Commun.* 21, 643–659.
30. Wu, S., and Shanks, R.A. (2004). Solubility study of polyacrylamide in polar solvents. *J. Appl. Polym. Sci.* 93, 1493–1499.
31. Miller-Chou, B.A., and Koenig, J.L. (2003). A review of polymer dissolution. *Prog. Polym. Sci.* 28, 1223–1270.
32. Mark, J.E. (2007). *Physical Properties of Polymers Handbook* (Springer).
33. Sperling, L.H. (2005). *Introduction to Physical Polymer Science* (John Wiley & Sons).
34. Wang, Z.L., and Wang, A.C. (2019). On the origin of contact-electrification. *Mater. Today* 30, 34–51.
35. Fan, F.-R., Tian, Z.-Q., and Lin Wang, Z. (2012). Flexible triboelectric generator. *Nano Energy* 1, 328–334.
36. Chen, A., Zhang, C., Zhu, G., and Wang, Z.L. (2020). Polymer materials for high-performance triboelectric Nanogenerators. *Adv. Sci.* 7, 2000186.
37. Shao, J., Jiang, T., and Wang, Z. (2020). Theoretical foundations of triboelectric nanogenerators (TENGs). *Sci. China Technol. Sci.* 63, 1087–1109.
38. Luo, J., and Wang, Z.L. (2020). Recent progress of triboelectric nanogenerators: From fundamental theory to practical applications. *EcoMat* 2, e12059.
39. Wang, Z.L. (2021). From contact electrification to triboelectric nanogenerators. *Rep. Prog. Phys.* 84, 096502.
40. Wang, Z.L. (2022). On the expanded Maxwell's equations for moving charged media system-General theory, mathematical solutions and applications in TENG. *Mater. Today* 52, 348–363.
41. Lin, S., Chen, X., and Wang, Z.L. (2022). Contact electrification at the liquid-solid interface. *Chem. Rev.* 122, 5209–5232.
42. Liu, C., and Bard, A.J. (2008). Electrostatic electrochemistry at insulators. *Nat. Mater.* 7, 505–509.
43. McCarty, L.S., and Whitesides, G.M. (2008). Electrostatic charging due to separation of ions at interfaces: contact electrification of ionic electrets. *Angew. Chem., Int. Ed. Engl.* 47, 2188–2207.
44. Šutka, A., Mālnieks, K., Lapčinskis, L., Kaufelde, P., Linarts, A., Bērziņa, A., Zābels, R., Jurķāns, V., Gorņevs, I., Blūms, J., and Knite, M. (2019). The role of intermolecular forces in contact electrification on polymer surfaces and triboelectric nanogenerators. *Energy Environ. Sci.* 12, 2417–2421.
45. Xu, C., Zi, Y., Wang, A.C., Zou, H., Dai, Y., He, X., Wang, P., Wang, Y.C., Feng, P., Li, D., and Wang, Z.L. (2018). On the electron-transfer mechanism in the contact-electrification effect. *Adv. Mater.* 30, 1706790.
46. Lin, S., Xu, L., Zhu, L., Chen, X., and Wang, Z.L. (2019). Electron transfer in nanoscale contact electrification: photon excitation effect. *Adv. Mater.* 31, 1901418.
47. Lin, S., Zheng, M., Luo, J., and Wang, Z.L. (2020). Effects of surface functional groups on electron transfer at liquid-solid interfacial contact electrification. *ACS Nano* 14, 10733–10741.
48. Fan, Y., Li, S., Tao, X., Wang, Y., Liu, Z., Chen, H., Wu, Z., Zhang, J., Ren, F., Chen, X., and Fu, E. (2021). Negative triboelectric polymers with ultrahigh charge density induced by ion implantation. *Nano Energy* 90, 106574.
49. Liu, Y., Mo, J., Fu, Q., Lu, Y., Zhang, N., Wang, S., and Nie, S. (2020). Enhancement of triboelectric charge density by chemical functionalization. *Adv. Funct. Mater.* 30, 2004714.
50. Shaw, P. (1917). Experiments on tribo-electricity. I.—The tribo-electric series. In *Proceedings of the Royal Society of London. Series A, Containing Papers of a Mathematical and Physical Character*, 94, pp. 16–33.
51. Zou, H., Guo, L., Xue, H., Zhang, Y., Shen, X., Liu, X., Wang, P., He, X., Dai, G., Jiang, P., et al. (2020). Quantifying and understanding the triboelectric series of inorganic non-metallic materials. *Nat. Commun.* 11, 2093–2097.
52. Seol, M., Kim, S., Cho, Y., Byun, K.E., Kim, H., Kim, J., Kim, S.K., Kim, S.W., Shin, H.J., and Park, S. (2018). Triboelectric series of 2D layered materials. *Adv. Mater.* 30, 1801210.
53. Yoo, D., Jang, S., Cho, S., Choi, D., and Kim, D.S. (2023). A Liquid Triboelectric Series. *Adv. Mater.* 35, 2300699.
54. Zamanpour, F., Shooshtari, L., Gholami, M., Mohammadpour, R., Sasanpour, P., and Taghavinia, N. (2022). Transparent and flexible touch on/off switch based on BaTiO₃/silicone polymer triboelectric nanogenerator. *Nano Energy* 103, 107796.
55. Diaz, A., and Felix-Navarro, R. (2004). A semi-quantitative tribo-electric series for polymeric materials: the influence of chemical structure and properties. *J. Electrost.* 62, 277–290.
56. Zheng, X., Zhang, R., and Huang, H. (2014). Theoretical modeling of relative humidity on contact electrification of sand particles. *Sci. Rep.* 4, 4399–4406.
57. Xu, C., Wang, A.C., Zou, H., Zhang, B., Zhang, C., Zi, Y., Pan, L., Wang, P., Feng, P., Lin, Z., and Wang, Z.L. (2018). Raising the working temperature of a triboelectric nanogenerator by quenching down electron thermionic emission in contact-electrification. *Adv. Mater.* 30, 1803968.
58. Fan, F.-R., Lin, L., Zhu, G., Wu, W., Zhang, R., and Wang, Z.L. (2012). Transparent triboelectric nanogenerators and self-powered pressure sensors based on micropatterned plastic films. *Nano Lett.* 12, 3109–3114.
59. Liu, Z., Li, S., Lin, S., Shi, Y., Yang, P., Chen, X., and Wang, Z.L. (2022). Crystallization-Induced Shift in a Triboelectric Series and Even Polarity Reversal for Elastic Triboelectric Materials. *Nano Lett.* 22, 4074–4082.
60. Lee, J., Chung, S.-H., Kim, B., Son, J.-h., Lin, Z.-H., Lee, S., and Kim, S. (2023). Wear and triboelectric performance of polymers with non-polar lubricants. *Tribol. Int.* 178, 108088.
61. Meng, Q., Zhang, M., Tang, R., Jin, W., Zhang, J., Lan, Z., Shi, S., Shen, X., and Sun, Q. (2022). Stretchable triboelectric nanogenerator with exteroception-visualized multifunctionality. *J. Mater. Chem. A Mater.* 10, 4300–4305.
62. Dai, S., Li, X., Jiang, C., Zhang, Q., Peng, B., Ping, J., and Ying, Y. (2022). Omnidirectional wind energy harvester for self-powered agro-environmental information sensing. *Nano Energy* 91, 106686.

63. Yan, K., Li, X., Wang, X.-X., Yu, M., Fan, Z., Ramakrishna, S., Hu, H., and Long, Y.-Z. (2020). A non-toxic triboelectric nanogenerator for baby care applications. *J. Mater. Chem. A Mater.* 8, 22745–22753.
64. Kim, H.-J., Yim, E.-C., Kim, J.-H., Kim, S.-J., Park, J.-Y., and Oh, I.-K. (2017). Bacterial nanocellulose triboelectric nanogenerator. *Nano Energy* 33, 130–137.
65. Annamalai, P.K., Nanjundan, A.K., Dubal, D.P., and Baek, J.-B. (2021). An overview of cellulose-based nanogenerators. *Adv. Mater. Technol.* 6, 2001164.
66. Wang, T., Li, S., Tao, X., Yan, Q., Wang, X., Chen, Y., Huang, F., Li, H., Chen, X., and Bian, Z. (2022). Fully biodegradable water-soluble triboelectric nanogenerator for human physiological monitoring. *Nano Energy* 93, 106787.
67. Wang, M., Li, W., You, C., Wang, Q., Zeng, X., and Chen, M. (2017). Triboelectric nanogenerator based on 317L stainless steel and ethyl cellulose for biomedical applications. *RSC Adv.* 7, 6772–6779.
68. Liu, Y., Fu, Q., Mo, J., Lu, Y., Cai, C., Luo, B., and Nie, S. (2021). Chemically tailored molecular surface modification of cellulose nanofibrils for manipulating the charge density of triboelectric nanogenerators. *Nano Energy* 89, 106369.
69. Ding, P., Chen, J., Farooq, U., Zhao, P., Soin, N., Yu, L., Jin, H., Wang, X., Dong, S., and Luo, J. (2018). Realizing the potential of polyethylene oxide as new positive tribo-material: Over 40 W/m² high power flat surface triboelectric nanogenerators. *Nano Energy* 46, 63–72.
70. Zhang, X., Huang, X., Kwok, S.W., and Soh, S. (2016). Designing non-charging surfaces from non-conductive polymers. *Adv. Mater.* 28, 3024–3029.
71. Liang, Q., Zhang, Q., Yan, X., Liao, X., Han, L., Yi, F., Ma, M., and Zhang, Y. (2017). Recyclable and green triboelectric nanogenerator. *Adv. Mater.* 29, 1604961.
72. Charoensuk, T., Pongampai, S., Pakawanit, P., and Vittayakorn, N. (2021). Achieving a highly efficient chitosan-based triboelectric nanogenerator via adding organic proteins: Influence of morphology and molecular structure. *Nano Energy* 89, 106430.
73. Charoensuk, T., Supansomboon, S., Pakawanit, P., Vittayakorn, W., Pongampai, S., Woramongkolchai, S., and Vittayakorn, N. (2022). Simple enhanced charge density of chitosan film by the embedded ion method for the flexible triboelectric nanogenerator. *Carbohydr. Polym.* 297, 120070.
74. Kim, H., Choi, S., Hong, Y., Chung, J., Choi, J., Choi, W.-K., Park, I.W., Park, S.H., Park, H., Chung, W.-J., et al. (2021). Biocompatible and biodegradable triboelectric nanogenerators based on hyaluronic acid hydrogel film. *Appl. Mater. Today* 22, 100920.
75. Lu, Y., Li, X., Ping, J., He, J.s., and Wu, J. (2020). A flexible, recyclable, and high-performance pullulan-based triboelectric nanogenerator (TENG). *Adv. Mater. Technol.* 5, 1900905.
76. Sarkar, P.K., Kamiya, T., and Acharya, S. (2019). Introduction of triboelectric positive bioplastic for powering portable electronics and self-powered gait sensor. *ACS Appl. Energy Mater.* 2, 5507–5514.
77. Zhang, J., Hu, Y., Lin, X., Qian, X., Zhang, L., Zhou, J., and Lu, A. (2022). High-performance triboelectric nanogenerator based on chitin for mechanical-energy harvesting and self-powered sensing. *Carbohydr. Polym.* 291, 119586.
78. Jiang, C., Zhang, Q., He, C., Zhang, C., Feng, X., Li, X., Zhao, Q., Ying, Y., and Ping, J. (2022). Plant-protein-enabled biodegradable triboelectric nanogenerator for sustainable agriculture. *Fundamental Research* 2, 974–984.
79. Bok, M., Lee, Y., Park, D., Shin, S., Zhao, Z.-J., Hwang, B., Hwang, S.H., Jeon, S.H., Jung, J.-Y., Park, S.H., et al. (2018). Microneedles integrated with a triboelectric nanogenerator: an electrically active drug delivery system. *Nanoscale* 10, 13502–13510.
80. Shin, S.-H., Kwon, Y.H., Kim, Y.-H., Jung, J.-Y., Lee, M.H., and Nah, J. (2015). Triboelectric charging sequence induced by surface functionalization as a method to fabricate high performance triboelectric generators. *ACS Nano* 9, 4621–4627.
81. Zhang, X.-S., Brugger, J., and Kim, B. (2016). A silk-fibroin-based transparent triboelectric generator suitable for autonomous sensor network. *Nano Energy* 20, 37–47.
82. Han, Y., Han, Y., Zhang, X., Li, L., Zhang, C., Liu, J., Lu, G., Yu, H.-D., and Huang, W. (2020). Fish gelatin based triboelectric nanogenerator for harvesting biomechanical energy and self-powered sensing of human physiological signals. *ACS Appl. Mater. Interfaces* 12, 16442–16450.
83. Li, L., Xin, Y., Wu, F., Lyu, X., Yao, Q., Yin, X., Zhang, Q., Shan, W., Chen, Y., and Han, Q. (2022). Electrospun hydrolyzed collagen from tanned leather shavings for bio-trioboelectric nanogenerators. *Polymers* 14, 5080–5086.
84. Zhang, Z., Gong, W., Bai, Z., Wang, D., Xu, Y., Li, Z., Guo, J., and Tung, L.-S. (2019). Oxygen-rich polymers as highly effective positive tribomaterials for mechanical energy harvesting. *ACS Nano* 13, 12787–12797.
85. Zhu, Z., Xia, K., Xu, Z., and Zhang, H. (2018). A triboelectric nanogenerator based on polypropylene carbonate and photoacid generator. *Solid State Electron.* 148, 16–19.
86. Wu, Y., Luo, Y., Qu, J., Daoud, W.A., and Qi, T. (2020). Nanogap and environmentally stable triboelectric nanogenerators based on surface self-modified sustainable films. *ACS Appl. Mater. Interfaces* 12, 55444–55452.
87. Gao, Y., Zhang, Y., Wang, X., Sim, K., Liu, J., Chen, J., Feng, X., Xu, H., and Yu, C. (2017). Moisture-triggered physically transient electronics. *Sci. Adv.* 3, e1701222.
88. Fu, S., Yang, G., Wang, J., Wang, X., Cheng, X., and Tang, R. (2017). Acid-degradable poly(ortho ester urethanes) copolymers for potential drug carriers: Preparation, characterization, in vitro and in vivo evaluation. *Polymer* 114, 1–14.
89. Yin, S., Xia, Y., Jia, Q., Hou, Z.-S., and Zhang, N. (2017). Preparation and properties of biomedical segmented polyurethanes based on poly(ether ester) and uniform-size diurethane diisocyanates. *J. Biomater. Sci. Polym. Ed.* 28, 119–138.
90. Lee, J.H., Yu, I., Hyun, S., Kim, J.K., and Jeong, U. (2017). Remarkable increase in triboelectrification by enhancing the conformable contact and adhesion energy with a film-covered pillar structure. *Nano Energy* 34, 233–241.
91. Luo, N., Xu, G., Feng, Y., Yang, D., Wu, Y., Dong, Y., Zhang, L., and Wang, D. (2022). Ice-based triboelectric nanogenerator with low friction and self-healing properties for energy harvesting and ice broken warning. *Nano Energy* 97, 107144.
92. Wang, C., Yokota, T., and Someya, T. (2021). Natural biopolymer-based biocompatible conductors for stretchable bioelectronics. *Chem. Rev.* 121, 2109–2146.
93. Ulery, B.D., Nair, L.S., and Laurencin, C.T. (2011). Biomedical applications of biodegradable polymers. *J. Polym. Sci. B Polym. Phys.* 49, 832–864.
94. Murthy, N., Wilson, S., and Sy, J. (2012). Biodegradation of polymers. *Polymer Science: A Comprehensive Reference* 10, 547–560.
95. Reeder, J.T., Xie, Z., Yang, Q., Seo, M.-H., Yan, Y., Deng, Y., Jinkins, K.R., Krishnan, S.R., Liu, C., McKay, S., et al. (2022). Soft, bioresorbable coolers for reversible conduction block of peripheral nerves. *Science* 377, 109–115.